Cell Transplantation, Vol. 26, pp. 351–364, 2017
Printed in the USA.

0963-6897/17 $90.00 + .00
DOI: https://doi.org/10.3727/096368916X692960
E-ISSN 1555-3892
www.cognizantcommunication.com

Adult-Derived Human Liver Stem/Progenitor Cells Infused 3 Days Postsurgery Improve Liver Regeneration in a Mouse Model of Extended Hepatectomy

Astrid Herrero,*† Julie Prigent,* Catherine Lombard,* Valérie Rosseels,* Martine Daujat-Chavanieu,‡ Karine Breckpot,§ Mustapha Najimi,* Gisèle Deblandre,* and Etienne M. Sokal*

*Université Catholique de Louvain, Institut de Recherche Expérimentale et Clinique (IREC), Pediatric Hepatology and Cell Therapy, Brussels, Belgium
†Department of Digestive Surgery and Liver Transplantation, Saint Eloi Hospital, Montpellier, France
‡Institut of Regenerative Medicine and Biotherapy (IRMB), Montpellier, France
§ Laboratory of Molecular and Cellular Therapy, Department of Physiology and Immunology, Medical School of the Vrije Universiteit Brussel (VUB), Brussels, Belgium

There is growing evidence that cell therapy constitutes a promising strategy for liver regenerative medicine. In the setting of hepatic cancer treatments, cell therapy could prove a useful therapeutic approach for managing the acute liver failure that occurs following extended hepatectomy. In this study, we examined the influence of delivering adult-derived human liver stem/progenitor cells (ADHLSCs) at two different early time points in an immunodeficient mouse model (*Rag2*$^{-/-}$*IL2R*$\gamma^{-/-}$) that had undergone a 70% hepatectomy procedure. The hepatic mesenchymal cells were intrasplenically infused either immediately after surgery ($n=26$) or following a critical 3-day period ($n=26$). We evaluated the cells' capacity to engraft at day 1 and day 7 following transplantation by means of human Alu qPCR quantification, along with histological assessment of human albumin and α-smooth muscle actin. In addition, cell proliferation (anti-mouse and human Ki-67 staining) and murine liver weight were measured in order to evaluate liver regeneration. At day 1 posttransplantation, the ratio of human to mouse cells was similar in both groups, whereas 1 week posttransplantation this ratio was significantly improved ($p<0.016$) in mice receiving ADHLSC injection at day 3 posthepatectomy (1.7%), compared to those injected at the time of surgery (1%). On the basis of liver weight, mouse liver regeneration was more extensive 1 week posttransplantation in mice transplanted with ADHLSCs (+65.3%) compared to that of mice from the sham vehicle group (+42.7%). In conclusion, infusing ADHLSCs 3 days after extensive hepatectomy improves the cell engraftment and murine hepatic tissue regeneration, thereby confirming that ADHLSCs could be a promising cell source for liver cell therapy and hepatic tissue repair.

Key words: Hepatic stem/progenitor cells; Mesenchymal cells; Xenotransplantation; Liver failure; Engraftment; Alu qPCR

INTRODUCTION

Over the last two decades, the incidence of malignant liver tumors in adults has been steadily increasing, with malignant liver tumors being at present the third leading cause of cancer mortality in the world [World Health Organization (WHO), 2008]. While these tumors can develop in normal livers, 80% of cases occur in livers affected by cirrhotic parenchyma or containing lesions induced by chemotherapy.

Surgical liver resection remains the gold standard of curative treatment for tumors in adults, enabling longer survival for treated patients. The postoperative mortality rate associated with major hepatectomies, defined as over three resected segments, has significantly decreased in recent years due to technological advances and improvements in preoperative patient selection and preparation. Nevertheless, the postoperative mortality rate remains high overall, between 3% and 5%, as reported in the scientific literature (7,14,15). Posthepatectomy liver failure (PHLF) has been shown to be a predominant cause of mortality after extensive liver resection, its incidence varying between 1.2% and 32% due to the heterogeneity of the population considered and lack of universally accepted PHLF definition (28). The little hepatic parenchymal tissue remaining postresection proves insufficient to produce the stimulus for regeneration that meets the

Received March 25, 2016; final acceptance October 24, 2016. Online prepub date: September 21, 2016.
Address correspondence to Professor Etienne M. Sokal, Cliniques Universitaires Saint-Luc, Paediatric Gastroenterology and Hepatology, Avenue Hippocrate 10, B-1200 Brussels, Belgium. Tel: +32-(0)2-7641387; Fax: +32-(0)2-7648909; E-mail: etienne.sokal@uclouvain.be

physiological requirements. Liver failure may subsequently induce acute multivisceral failures and eventually result in death. Under certain conditions, PHLF can be treated using orthotopic liver transplantation, though indications are quite restricted, while it remains difficult to make a decision that is sufficiently early to be of benefit (10,24). The use of artificial liver support devices [e.g., molecular adsorbent recirculating system (MARS)] (33) has also proven effective, enabling clinical improvements in jaundice and hepatic encephalopathy, as well as reducing portal hypertension. Yet improvements are mostly of short duration, with no clear benefits on long-term survival shown.

Given this setting, liver cell therapy appears to be an appealing alternative strategy for PHLF management. Transplantation of hepatocytes in both animal models (1,11) and humans (8) has revealed the cells' ability to engraft in the recipient liver while supplying metabolic functions.

Nevertheless, donor shortage, difficulties in cell culture processes, as well as cell damage caused by cryopreservation together present limiting factors for the routine transplantation of hepatocytes. Other cell sources, such as stem or progenitor cells, offer distinct advantages over mature liver cells, owing to their capacities to proliferate well in vitro and to withstand cryopreservation. A growing interest in these cells has emerged from the accumulating evidence of their involvement in both tissue regeneration and repair. We have previously isolated and characterized adult-derived human liver stem/progenitor cells (ADHLSCs) from livers of cadaveric donors (21). These cells emerge from the in vitro culture of the parenchymal fraction obtained after collagenase perfusion of the liver and centrifugation to remove the nonparenchymal cells (duct cells, stellate cells, and sinusoidal endothelial cells). The in vitro culture allows for the removal of hepatocytes, which dedifferentiate and die, and other contaminating cells, leading to the enrichment of the progenitor cells, which possess both mesenchymal and hepatic characteristics. Despite some degree of heterogeneity, our previous research has shown the absence of hematopoietic and biliary markers. These cells are therefore different than the cells described by Huch et al., which are of ductal origin and express cytokeratin 19 (CK19) (13). ADHLSCs present significant advantages over hepatocytes, which have been previously proposed for use in cell therapy: (i) potential to proliferate and differentiate into hepatocyte-like cells (21); (ii) resistance to cryopreservation; and (iii) capacity to proliferate and differentiate in vivo so as to promote liver regeneration when infused via the intrasplenic route in severe combined immunodeficiency (SCID) mice following partial 20% hepatectomy (16).

In our study, we investigated the engraftment success of ADHLSCs and their capacity to improve liver regeneration in immunosuppressed mice following significant hepatectomy (70% resection), comparing two groups infused at two different time points postsurgery. In the early phase following an extensive hepatectomy procedure, inflammation and microvascular disturbances were predominant features (40). However, at 72 h posthepatectomy, numerous growth factors, such as hepatocyte growth factor (HGF) and vascular endothelial growth factor (VEGF), were shown to be upregulated while promoting vascularization (20). These inductive angiocrine signals secreted by sinusoidal endothelial cells are paramount to regeneration in the remnant liver tissue (6). We have hence proposed to evaluate whether progenitor stem cells should be injected either before or after this critical period to be able to provide the best improvement possible in engraftment and liver regeneration. We have thus chosen to compare cell injection immediately following hepatectomy, potentially limiting the surgical procedure while being less invasive for the patient, with injection carried out 3 days postsurgery, potentially benefiting from a better environment with local proliferation signals.

MATERIALS AND METHODS

This study was accepted by the institution's ethics review board (comité d'éthique hospitalo-facultaire) (reference JMM/sy/2010/12) for the use of human-derived tissue, with appropriate informed consent obtained from all tissue donors. In addition, the animal experiments were approved by the ethics committee for animal experimentation of the Université Catholique de Louvain Health Sciences Department (reference 2012/UCL/MD/009).

Animals

Recombination activating gene 2 null, interleukin 2 receptor γ chain null (*Rag2*$^{-/-}$*IL2R*$\gamma^{-/-}$) transgenic male mice, aged 8 to 10 weeks and weighing 20 to 25 g, were purchased from Taconic (Hudson, NY, USA). They were dealt with in accordance with the guidelines for human care pertaining to laboratory animals established by the Université Catholique de Louvain in line with European Union regulation and protocols, as approved by the local ethics committee. All mice were bred with an alternating 12:12-h light/dark cycle under monitored temperature conditions, with free access to standard food and water. These mice lacked T, B, and NK cells, thus constituting extremely useful subjects for xenogenic stem cell transplantation (5).

Partial Hepatectomy Procedure

All operative procedures were performed under general anesthesia using 2% isoflurane (Forane®; Abbott GmbH & Co, Wiesbaden, Germany) and 1% oxygen. The mice were placed on a 37°C heating plate throughout the perioperative period. The abdominal wall was sterilized using a surgical scrub, and a transverse incision was

made. Following the technique described by Makino et al. (19), a 70% hepatectomy was performed by removing separately, after placing a selective vascular ligature (Prolene, 6.0 silk; Ethicon, San Lorenzo, Puerto Rico), the right anterior lobe, left anterior lobe, and the left posterior lobe, respectively. Isotonic saline solution (0.9%) (B. Braun Medical, Diegem, Belgium) was administered onto the intraperitoneal organs throughout the surgical procedure in order to prevent dehydration. After abdominal closure, an analgesic solution (Temgesic) (0.1 mg/kg/12 h) (Reckitt Benckiser, Anderlecht, Belgium) and a 0.9% NaCl solution were subcutaneously injected into the mice. The pain, weight, and behavior of the mice were monitored daily following surgery. Analgesic and hydration solutions were systematically provided by subcutaneous injection from the day following surgery on a case-by-case basis over the following days.

Animal Study Design and In Vivo Procedure

In a preliminary study, 70% hepatectomies were performed on 50 mice (25 wild type and 25 immunosuppressed) in order to evaluate the general condition of the animals following surgery. Liver function and regeneration were assessed via quantification of serum transaminases and bilirubin and by anti-Ki-67 immunohistochemistry, respectively. In the study presented here, 52 *Rag2*$^{-/-}$*IL2R*$\gamma^{-/-}$ mice were hepatectomized and divided into two groups (Fig. 1). Group A animals were injected intrasplenically immediately following hepatectomy; group B animals received the injection 3 days posthepatectomy during a second surgical intervention.

Cell Transplantation Procedure

Two types of cells were injected: 1) ADHLSCs (one donor) or 2) fresh human hepatocytes (one donor) (as gold standard). The cells were suspended in phosphate-buffered saline (PBS) (Lonza, Braine-l'Alleud, Belgium) supplemented with 4% *N*-acetylcysteine (NAC) (Lysomucil®; Zambon, Vicenza, Italy) (formulation medium used to modulate the procoagulant activity induced by cell infusion). A sham group was added for each corresponding experimental condition with the same formulation medium without any cells. To assess cell engraftment, two time points were chosen for animal sacrifice: 1) 24 h after cell injection to evaluate treatment retention while observing changes in liver architecture induced by surgery, along with the mechanical effects of cell injection; 2) 7 days after cell injection to assess both the actual engraftment rate and liver regeneration. At time of sacrifice, the blood, liver, spleen, and lungs were removed and preserved in specific conditions: either fixed in 3.5% formaldehyde (Sigma-Aldrich, Diegem, Belgium) overnight and embedded in paraffin or snap frozen and stored at −80°C. The animals and remnant liver tissue were weighed, with liver mass quantified.

Culture of eGFP$^+$ ADHLSCs for Infusion

ADHLSCs were isolated, as described by Najimi et al. (21), from livers of cadaveric donors. In the current study, cells derived from a single male donor, aged 1 week, were cultured in Dulbecco's modified Eagle's medium (DMEM) supplemented with 10% fetal bovine serum (FBS) and 1% penicillin–streptomycin on cell bind dishes (all from Life Technologies, Ghent, Belgium). Our

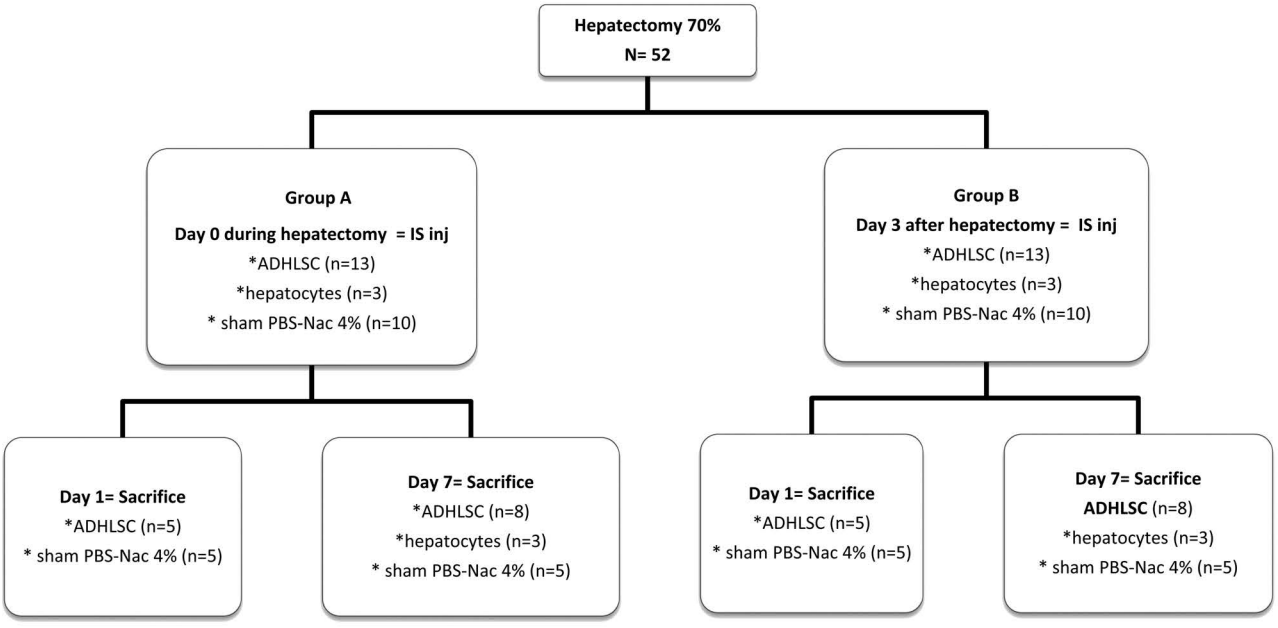

Figure 1. Animal study design.

study was accepted by the institution's ethical review board for the use of human-derived tissue, with appropriate informed consent received from all tissue donors.

To facilitate cell tracking and evaluate cell engraftment efficiency, ADHLSCs were transduced at the third culture passage by a lentivirus expressing the enhanced green fluorescent protein (eGFP) (gift from Dr. Karine Breckpot, Vrije Universiteit, Brussel, Belgium). The transduced cells were thawed and cultured 7 days before injection to ensure the transplantation of proliferative cells. These cells were characterized beforehand to ensure that their phenotype had not been altered by viral transduction. In this regard, we ensured that the viability, growth rate of the transfected cells, as well as their pattern of expression of characteristic markers ($CD73^+$, $CD90^+$, $CD29^+$, $CD44^+$, $CD117^-$, and $CD133^-$) and their capacity to differentiate into hepatocyte-like cells when subjected to a hepatogenic differentiation protocol in vitro were the same as those of the untransfected cells (21). Overall 1 million nondifferentiated $eGFP^+$ ADHLSCs were suspended in 100 µl of PBS 4% NAC for injection.

Transaminase (ASAT and ALAT) Levels and Serum Bilirubin Titration

Serum levels of alanine aminotransferase (ALAT) and aspartate aminotransferase (ASAT), as well as total and conjugated bilirubin were measured via the Synchron® lab automated system (Etten-Leur, The Netherlands) in peripheral blood collected before sacrifice. The required sample volumes were 23 µl for ASAT and ALAT dosage, and 10 µl for bilirubin dosage.

Cell Detection and Quantification

Alu qPCR Assay. Human cells were quantified by Alu-primed quantitative polymerase chain reaction (Alu qPCR) assay, as previously described (26). Tissue samples were first disrupted using FastPrep® Lysing Matrix D (MPbio, Brussels, Belgium), and then genomic DNA was extracted using the QIAamp DNA Tissue Mini Kit (Qiagen, Hilden, Germany). DNA concentration and quality were assessed by absorbance (NanoDrop; Thermo Scientific, Erembodegem, Belgium) and verified by qPCR assay using the mouse β-actin gene (forward: 5′-AAGGCCAACCG TGAAAAGAT-3′ and reverse: 5′-GTGGTACGACCAG AGGGATAC-3′) (Invitrogen, Erembodegem, Belgium). The PCR was performed on a LightCycler 480 (Roche Diagnostics, Penzberg, Germany) in a total volume of 25 µl containing the LC480 SYBR Green I Master Mix (1×) (Roche Diagnostics), 0.15 µM of each AluYb8 primer (forward: 5′-CGAGGCGGGTGGATCATGAGGT-3′ and reverse: 5′-TCTGTCGCCCAGGCCGGACT-3′) (Invitrogen), and 100 ng of DNA. Two negative controls lacking DNA templates were processed in each PCR plate to ensure the assay was free of contamination. The results were analyzed using LC480 software following the second derivative method according to the MIQE guidelines for qPCR (Minimum Information for Publication of Quantitative Real-Time PCR Experiments) (3).

Tissue samples from the livers and spleens were harvested from two different locations within the organs, subjected to two independent DNA extraction procedures, and then further analyzed in triplicate using qPCR. The approximate hepatic cell number within 25 mg of liver tissue was extrapolated on the basis of the figure of 50×10^6 hepatic cells/g of liver mass (39) or 1.25×10^6 mice cells/25 mg. Quantification of human cells was established on the basis of cell mixing standard curves (10^5 to 50 ADHLSCs added to hepatic mouse cells in order to obtain 10^6 total cells per sample) according to Cq value for AluYb8 amplification (26). Linear regression model showed an excellent determination coefficient ($R^2>0.99$) and a slope of −3.78, corresponding to an efficiency of 83.9%. Human cell percentages were thus calculated as the ratio of the number of human cells to an estimated number of 1.25×10^6 mouse cells.

Histological Analysis

Histological analyses were performed in the harvested liver tissue at the time of sacrifice on 4-µm sections by immunohistochemistry. To detect ADHLSCs, several antibodies were used: anti-human albumin (A6684; 3 µg/ml; Sigma-Aldrich), anti-α-SMA (M0851; 0.7 µg/ml; Dako, Heverlee, Belgium), anti-vimentin (10515; 1/50; Progen, Heidelberg, Germany), anti-OTC (HPA000243; 0.8 µg/ml; Sigma-Aldrich), and anti-GFP (ab290; 1/50; Abcam Inc., Cambridge, MA, USA). To detect hepatocytes, antibodies against human albumin and ornithine transcarbamylase (OTC) were employed. Paraffin-embedded liver sections were stained with the M.O.M. Immunodetection Kit (avidin–biotin amplification system from Vector Laboratories Inc., Burlingame, CA, USA) for albumin, α-smooth muscle actin (α-SMA), and vimentin detections and the EnVision anti-rabbit system (Dako) for OTC and GFP. Staining was revealed by either fluorescence or diaminobenzidine (DAB) substrate (Dako). The slides were then counterstained with 4′,6-diamidino-2-phenylindole (DAPI; D9542; 4 µg/ml; Sigma-Aldrich) or Mayer's hematoxylin (MHS80-2.5L; Sigma-Aldrich), and then further coverslipped with ProLong® Gold Antifade Reagent (Invitrogen) or Entellan mounting medium (Merck, Overijse, Belgium), respectively. The sections were examined under normal light microscopy or epifluorescence using a Zeiss Axio Imager ZI fluorescent microscope and 20× objective. The images were analyzed using the AxoVision 4.8 software (Zeiss, Zaventem, Belgium).

Analysis of Liver Regeneration

Regenerated Liver Weight. The restitution of liver weight was calculated as the percentage of regenerated liver mass using the following equation: $100\times(C-[A-B])/A$, where A is the estimated total liver weight at the time of resection (5% of body weight), B is the excised liver weight, and C is the weight of the regenerated liver at the time of sacrifice (23).

Proliferation Evaluation by Ki-67 Immunostaining. The endogenous mouse liver regeneration was analyzed by immunostaining using a rat anti-mouse Ki-67 primary antibody (M7249; 0.7 µg/ml; Dako). The signal was visualized using an avidin–biotin–peroxidase amplification system, as described above. The proliferation of the injected human cells was evaluated using a mouse anti-human Ki-67 primary antibody (M7240; 0.7 µg/ml; Dako) along with the M.O.M. Kit. The images were captured, and labeled cell area was manually quantified by two independent operators using the ImageJ software [National Institutes of Health (NIH), Bethesda, MD, USA], each time taking three different sections of three different fields centered on a portal space.

Statistical Analysis

All the findings were expressed as mean ± standard error of the mean (SEM) (22). Statistical analyses were performed using GraphPad Prism® (La Jolla, CA, USA). Comparisons between the two groups were performed by means of Student's *t*-test. One-factor analysis of variance (ANOVA) was applied, with the Newman–Keuls post hoc test used for multiple comparisons between more than two groups. Differences were considered statistically significant when the following p values were found: $p<0.05$, $p<0.01$, $p<0.001$.

RESULTS

Preliminary Study Results for the 70% Hepatectomy Model

The results of the 70% hepatectomy model revealed a critical period consisting of the first 2 days posthepatectomy where the mice were in poor general condition, with significant weight loss and impaired liver function (data not shown). These observations concur with the data obtained by macroscopic and microscopic liver analyses, displaying signs of ischemia and vacuolar degeneration with steatosis during this period (Fig. 2). Similar results were reported in the immunosuppressed mice group. Moreover, from day 3 posthepatectomy onward, no more signs of vasoconstriction or steatosis were observed (Fig. 2). Ki-67 immunostaining revealed a maximal percentage of mouse liver cell regeneration at day 3 (data not shown). These findings thereby justified the choice of using day 3 posthepatectomy as an optimal time point of cell injection for all future studies.

Animal Survival Rate After Cell Transplantation Associated With Extensive Hepatectomy

All the mice that underwent 70% hepatectomy, whether from group A (injected immediately after surgery) or group B (injected 3 days postsurgery) survived for up to 24 h after cell injection ($n=10$), until the first sacrifice time point at day 1 postsurgery. No deaths occurred during the surgical procedure. All the group B mice ($n=8$ for ADHLSCs; $n=3$ for hepatocytes) survived for 1 week, until the second sacrifice time point at day 7. In contrast, three mice from group A injected with ADHLSCs ($n=8$; 37%) and one injected with hepatocytes ($n=3$; 33%) died on days 2 and 3 posthepatectomy, respectively. No clinical disturbances were observed after the cells' injection via the intrasplenic route during the second intervention in group B. On the other hand, the group A mice began to recover from anesthesia and surgery approximately 3 h posthepatectomy, regaining within 48 h approximately the same activity as observed preoperation. Weight loss in group A was significantly higher than that in group B (9% of initial body weight vs. 17% at day 2 postsurgery; $p<0.02$). The animals that died exhibited no jaundice or ascites. The liver tissue was necrotized, yet lungs were normal on macroscopic analysis at autopsy.

In the sham groups, no mice died following vehicle injection. We thus conclude that delaying cell injection to day 3 postoperation appears to be associated with less mortality than injecting cells immediately following surgery.

Hepatic Enzyme Levels in Postsurgery Injected Mice After Cell Transplantation

Serum ALAT and ASAT are hepatic enzymes that are released into the bloodstream upon hepatic damage. ALAT and ASAT levels were significantly higher in group A than in group B or the sham group, measured 24 h after cell injection ($p<0.05$). However, 7 days after injection, there was no difference between the different groups, with normal values recovered in all (Fig. 3A and B). At days 1 and 7, serum direct bilirubin (mg/ml) did not significantly differ between the groups (Fig. 3C).

Human Cell Quantification in Mouse Liver Tissue

After having optimized the 70% hepatectomy murine model, experimental groups were set to assess engraftment as follows (Fig. 1).

In group A, all animals were injected with cells via the intrasplenic route immediately after 70% hepatectomy, with 13 receiving 1×10^6 ADHLSCs.

Five mice were sacrificed 1 day following transplantation. The proportion of ADHLSCs reached 2.14% to

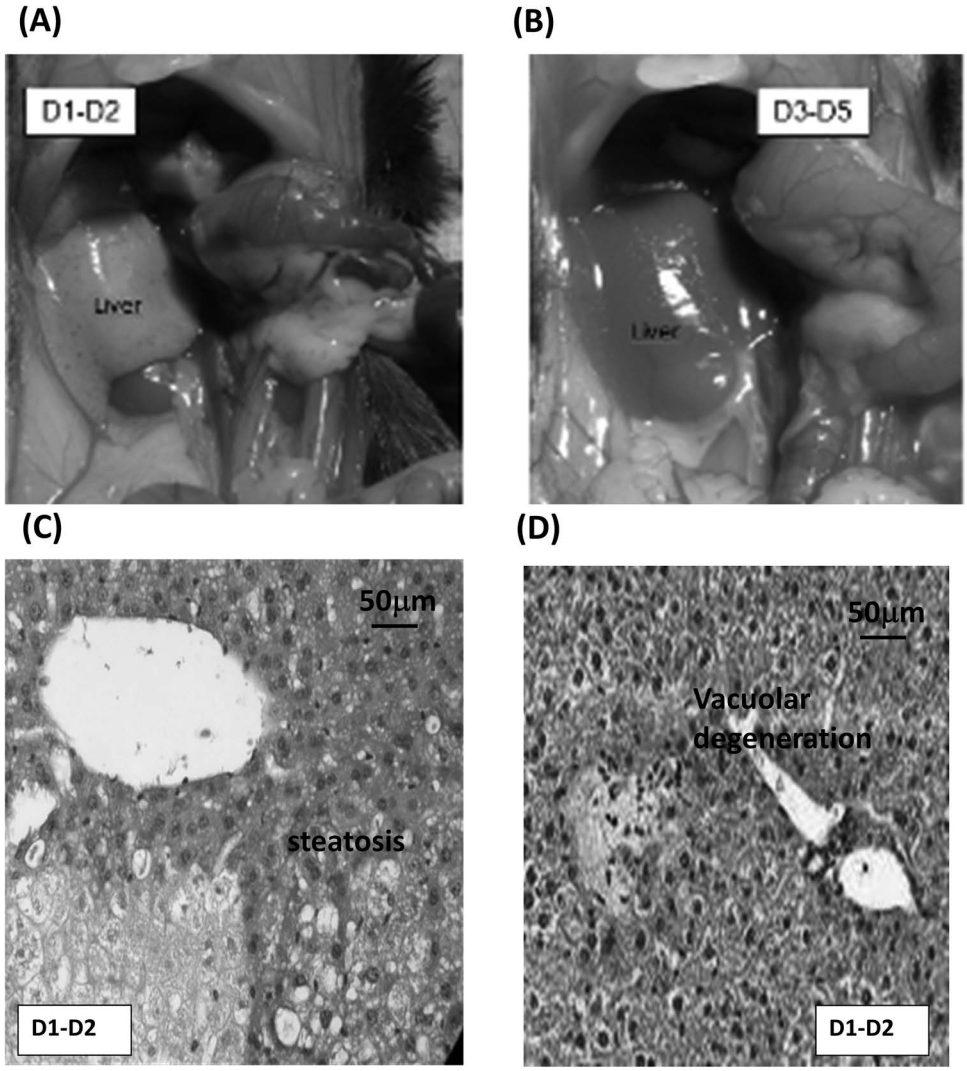

Figure 2. Macro- and microscopic analysis of remnant liver tissue after 70% hepatectomy. (A, B) Representative macroscopic images of remnant liver tissue on days 1 and 2 (A) or days 3 through 5 (B) post 70% hepatectomy. (C, D) Representative example of the microscopic analysis results obtained on days 1 and 2 showing steatosis (C) and vacuolar degeneration (D).

3.88% of total liver cells (between 26,750 and 47,500 ADHLSCs measured in 25 mg of mouse liver tissue). Eight mice were sacrificed 7 days after transplantation (only five were analyzed because of three deaths in this group). The ADHLSCs proportion reached 0.66% to 1.71% of total cells (between 8,200 and 21,375 ADHLSCs measured in 25 mg of mouse liver tissue). The relative percentage of ADHLSCs to mouse liver cells decreased significantly between days 1 and 7 (2.53% vs. 1.00%; $p=0.003$) (Fig. 4A).

In comparison, in three mice transplanted with 1×10^6 hepatocytes, the proportion of detected human cells represented 0.13%–0.85% of the total mouse cells. Sham group mice exhibited no detectable human DNA signals. All group B animals were transplanted with cells via the intrasplenic route on day 3 post 70% hepatectomy, 13 with 1×10^6 ADHLSCs. Five mice were sacrificed on day 1 posttransplantation. The ratio of ADHLSCs to mouse cells ranged from 1.20% to 2.18% (between 15,000 and 27,250 ADHLSCs measured in 25 mg of mouse liver tissue). Eight mice were sacrificed 1 week posttransplantation. The ADHLSCs count was 1.03% to 2.15% of the total cells (between 12,875 and 26,875 measured in 25 mg of mouse liver tissue). The proportion of ADHLSCs in the mouse liver did not significantly differ between days 1 and 7 (1.88% vs. 1.70%; $p=0.48$) (Fig. 4B). The proportion of hepatocytes on day 7 posttransplantation was analyzed in three mice, with 0.16%, 0.76%, and 1.80% found, respectively. Again, none of the sham group mice exhibited detectable human DNA signals.

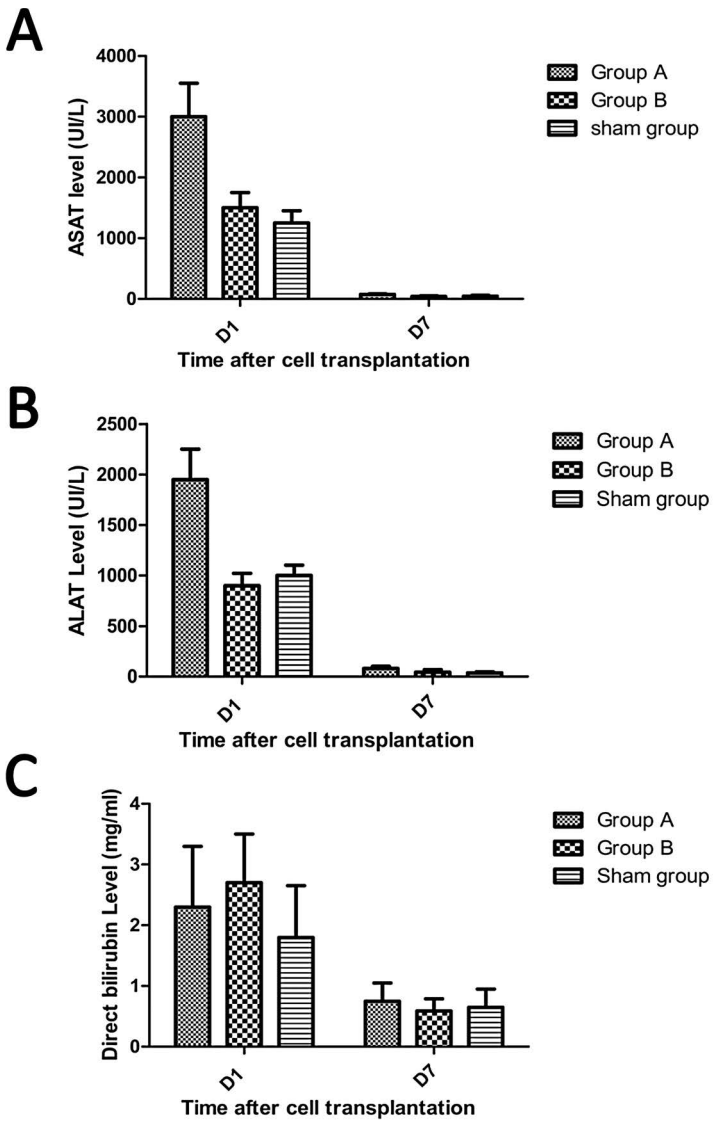

Figure 3. Hepatic enzyme levels in serum posthepatectomy and after ADHLSCs transplantation. Peripheral blood was collected from the mice just before sacrifice on day 1 and day 7 posttransplantation with ADHLSCs. Serum levels of aspartate aminotransferase (ASAT) (A), alanine aminotransferase (ALAT) (B), and direct bilirubin (C) were measured via the Synchron® system. ADHLSCs, adult-derived human liver stem/progenitor cells.

When comparing the proportion of ADHLSCs between the two groups, we found it did not significantly differ 24 h posttransplantation (2.53% vs. 1.88%; $p = 0.107$) (Fig. 4C), whereas it was significantly higher in group B than in group A (1.70% vs. 1.00%; $p = 0.016$) (Fig. 4D) on day 7 posttransplantation.

In the spleen, between 1,445 and 7,500 human cells were found 24 h after transplantation, though no more cells could be detected after 7 days (lower signal under the quantification limit), with no significant differences found between the two groups. The signal emanating from the lungs was also below the assay detection limit on day 7 posttransplantation.

Localization of the Migration and Engraftment of Transplanted Human Cells

Prior to transplantation, we verified that the transduction of the cells (with eGFP) to be injected did not affect their original phenotype and functionality in vitro. Immunohistochemistry analyses using antibodies specific to eGFP (Fig. 5A) and human albumin (Fig. 5B), as well as α-SMA (Fig. 5C), revealed the in vivo presence of ADHLSCs, along with the maintenance of their phenotype within the tissue. On day 1 posttransplantation, migrating individual ADHLSCs or hepatocytes were already observed in recipient liver tissues, primarily in the vascular structures around the periportal spaces, while on

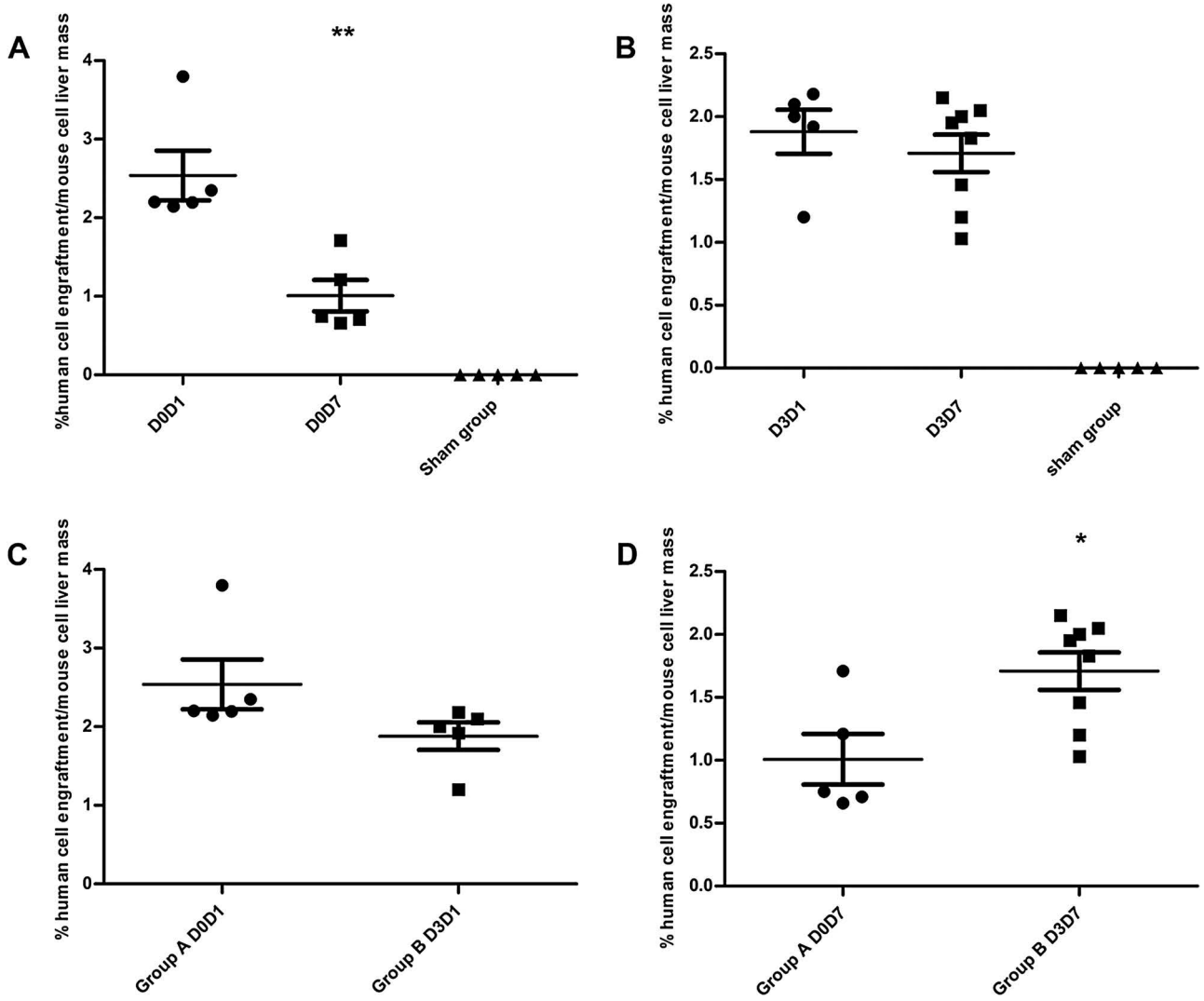

Figure 4. Quantification of ADHLSCs in mouse liver tissue at days 1 and 7 following transplantation. Results of AluYb8 qPCR assay performed in triplicate with 100 ng of DNA extracted from 25-mg samples from mice liver tissue in group A (A), showing a significant decrease between days 1 (group labeled D0D1) and 7 (group labeled D0D7) following cell transplantation ($p=0.003$); and in group B (B), showing stable level of human cells in mice liver tissue. (C, D) Comparison of data from groups A and B obtained on day 1 (C) and day 7 (D) following transplantation and exhibiting significant differences ($p=0.016$). ADHLSCs, adult-derived human liver stem/progenitor cells; PCR, polymerase chain reaction.

day 7 posttransplantation, cells were found entering the mouse liver parenchyma. Vimentin, OTC, and CK8–18 immunostaining on liver sections transplanted with ADHLSCs was negative on days 1 and 7, yet positive on those transplanted with hepatocytes (data not shown). There was no difference between groups A and B in terms of localization and morphology of the transplanted cells. However, we observed more significant liver injuries in group A, with vacuolar degeneration and several zones of ischemia still present at day 7, in comparison with group B. No necrotic lesions were observed in either the sham groups or group B. In addition, there was no macroscopic evidence of thrombosis.

Impact of Cell Transplantation on Mouse Liver Regeneration

On the basis of liver weight analysis, the regeneration rate was not significantly different between the transplanted mice and the sham group mice from groups A (2.7±1.48% vs. 1.16±0.9%) and B (27±1.58% vs. 28.7±1.22%) at day 1 posttransplantation. However, at day 7, the regeneration rate was significantly higher in the mice transplanted with ADHLSCs than in the sham group mice from groups A (43.4±2.1% vs. 20.20±1.6%; $p<0.0001$) and B (65.31±2.09% vs. 42.7±1.17%; $p<0.0001$) (Fig. 6A).

These data were further confirmed by visualizing liver tissue proliferation via immunohistochemical staining

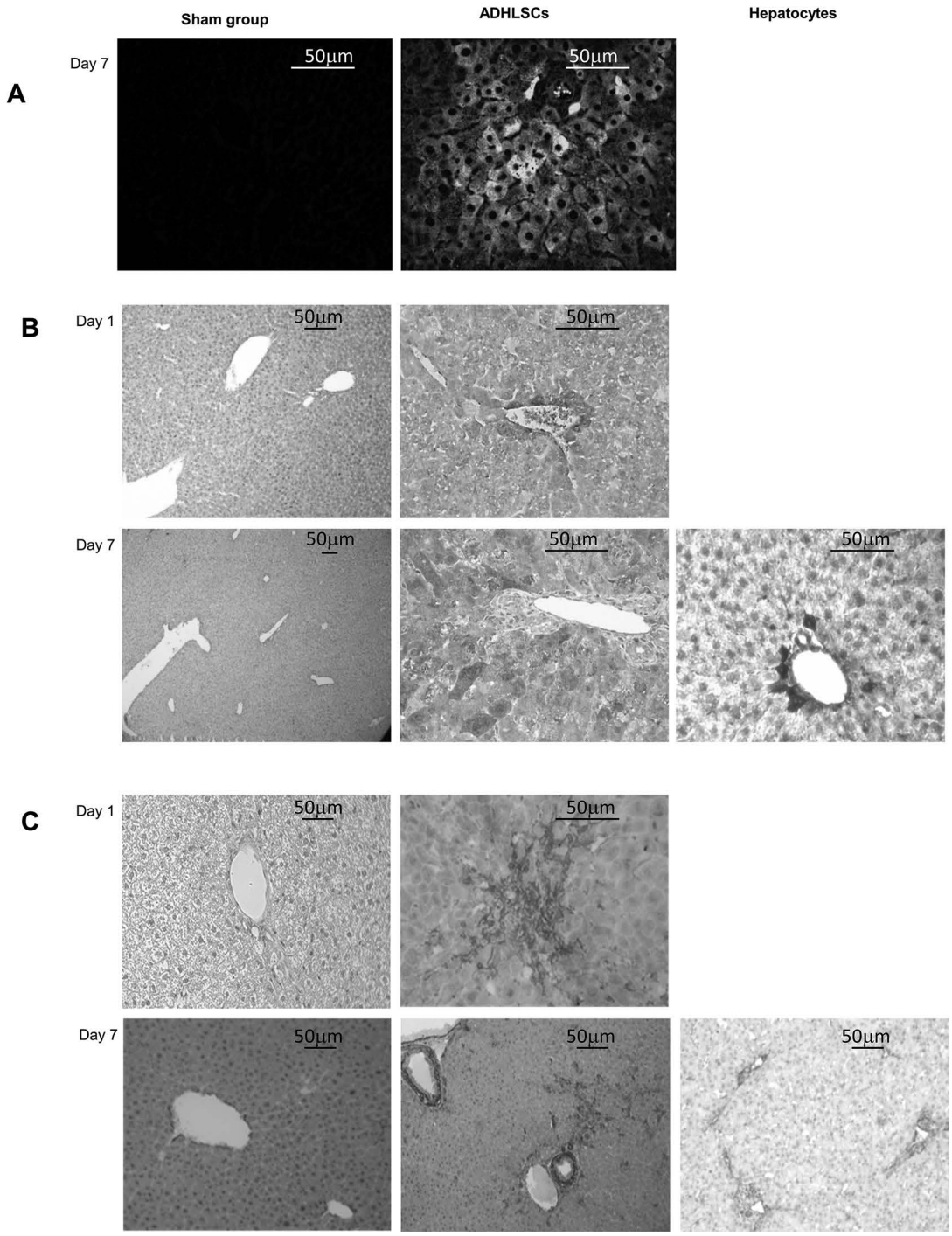

Figure 5. Visualization of the human cells implanted in mouse livers by immunohistochemistry. (A) Representative result of the tracking of eGFP$^+$ ADHLSCs in mouse liver tissue by direct fluorescence microscopy. Implantation of human cells in group B is visible 7 days after injection, with cells primarily located around the periportal spaces and starting to enter the parenchyma. (B) Representative result of the anti-human albumin immunostaining. Liver sections from mice transplanted with ADHLSCs and the sham group were analyzed on days 1 and 7 following transplantation (only on day 7 for hepatocytes). One day after transplantation, human albumin-positive ADHLSCs were only found implanted near the periportal spaces. Seven days after injection, human cells had migrated in the liver parenchyma. (C) Representative result of the anti-human α-smooth muscle actin (α-SMA) immunostaining. Liver sections from mice transplanted with ADHLSCs and the sham group were analyzed on days 1 and 7 following transplantation (only on day 7 for hepatocytes). α-SMA$^+$ cells were detected in the mice injected with ADHLSCs, confirming the results obtained with the anti-human albumin staining, whereas no α-SMA$^+$ cells were detected in the mice injected with hepatocytes, since these cells are α-SMA$^-$. ADHLSCs, adult-derived human liver stem/progenitor cells.

of mouse Ki-67 (Fig. 6C). At day 1 posttransplantation, the same percentage of positively stained cells was observed in both the sham group mice and those transplanted with ADHLSCs, with 8% and 33% of Ki-67$^+$ cells observed in groups A and B, respectively (Fig. 6B). Conversely, at day 7 posttransplantation, the percentage of Ki-67$^+$ mouse cells was significantly higher in the ADHLSC-transplanted mice than in the sham group or hepatocyte-transplanted mice in both groups A ($28 \pm 3.4\%$ vs. $13 \pm 2.7\%$ vs. $16 \pm 3.2\%$; $p < 0.01$) and B ($25 \pm 2.5\%$ vs. $5 \pm 1.2\%$ vs. $10 \pm 2.1\%$; $p < 0.01$), respectively (Fig. 6B).

On the other hand, immunohistochemical staining of human Ki-67 was negative in all sections analyzed in each group, demonstrating that ADHLSCs trigger liver regeneration by inducing endogenous liver cell proliferation.

DISCUSSION

This study primarily sought to evaluate the capacity of ADHLSCs to engraft in liver tissue via intrasplenic administration, as well as their ability to increase hepatic regeneration, in a mouse model of 70% hepatectomy, a well-known liver regeneration model (19,32). In particular, our work's originality resided in its comparison of different cell injection timings following the hepatectomy procedure. The underlying hypothesis was that performing cell transplantation in the aftermath of the critical first 2 postsurgery days (when ischemia and microvascular damages may occur) likely improves survival and engraftment of human cells in the mouse liver.

We demonstrated that injecting ADHLSCs on the third day after hepatectomy, instead of immediately after the procedure, significantly improved the percentage of human-to-mouse cell proportions in the liver, measured 1 week after transplantation (1.7% vs. 1%; $p < 0.016$), while the quantity of implanted cells had not yet differed at just 1 day after transplantation. Furthermore, the presence of hepatic necrosis and vacuolar degeneration observed in group A, yet absent in group B and the sham groups, illustrates the significant damage that can be caused to hepatic tissue by simultaneously combining extensive hepatectomy along with cell transplantation. These results concur with increased hepatic enzymes (ALAT and ASAT) detected in group A 24 h posttransplantation and the high mortality rate found in group A (36%) versus the absence of deaths in the sham groups or group B. Interestingly, we noted a similar impact on liver regeneration in both groups despite a higher percentage of cells engrafted in group B. One could wonder what would happen in an extended hepatectomy model where over 70% of the liver is removed. It is likely that in such model, designed to test survival rather than regeneration, the survival of the mice would be worse in group B, as mortality usually occurs within 48 h posthepatectomy.

Moreover, our current results demonstrate an increase in human-versus-mouse cell proportions. This observation is contrary to the findings of previous investigations from our laboratory using a 20% hepatectomy model in SCID mice (16), where the percentage of human-to-mouse cells was less than 0.5% 1 week posttransplantation. This improvement could be attributable to two primary factors: 1) increased regeneration stimulus in the 70% hepatectomy model; 2) use of a more immunosuppressed mouse model (*Rag2*$^{-/-}$*IL2*$\gamma^{-/-}$).

Our findings concur with results from other groups published in the scientific literature (4). Cells transplanted by intrasplenic route migrated in the liver quickly, integrating with the parenchyma as early as 1 day after infusion. A small number of cells were still retained in the spleen 24 h posttransplantation, yet had disappeared after day 7. No migration into the pulmonary system was found. A crucial point to consider is that liver cells are large in size (15–30 μm), with the size-to-structure relationship between transplanted cells and hepatic sinusoids consequently being a crucial factor likely to influence cell integration into the parenchyma (30). One typical outcome of extensive hepatectomy is ischemia–reperfusion syndrome, triggering inflammatory damage and microvascular constriction in the remaining liver tissue (17,18). This was clearly evidenced at the macroscopic level by the liver's pale aspect at that time point. Of note is that these phenomena were still reversible within the first 72 h. Such parameters could impact, in a mechanical way, cell distribution and account for the improvement in engraftment observed in group B, whose animals underwent the later injection after hepatectomy. Moreover, transplanted cells may have benefited from angiocrine signals that only appear 72 h posthepatectomy (6). In addition, a large proportion of transplanted cells were likely cleared early after transplantation due to the major hypoxia induced immediately following liver resection and in the first days thereafter. Nevertheless, this particular phenomenon may not, of course, occur when the injection is delayed. The low engraftment rate could theoretically also be explained by instant blood-mediated inflammatory reaction (IBMIR) provoked by cell infusion, as described in the literature (35). Adding an anticoagulant cocktail to the cell infusion solution could prove valuable, improving the survival rate of transplanted cells while positively influencing their engraftment (34). Additionally, novel strategies, such as the development of grafts composed of human stem cells embedded in a mix of growth factors and extracellular matrix biomaterials or, alternatively, cotransplantation with endothelial cells, have produced encouraging results (12,37).

In our 70% hepatectomy model, mouse liver regeneration was faster and more significant in mice transplanted with ADHLSCs than in either the sham group or the group transplanted with hepatocytes. Growing evidence published in the scientific literature suggests that

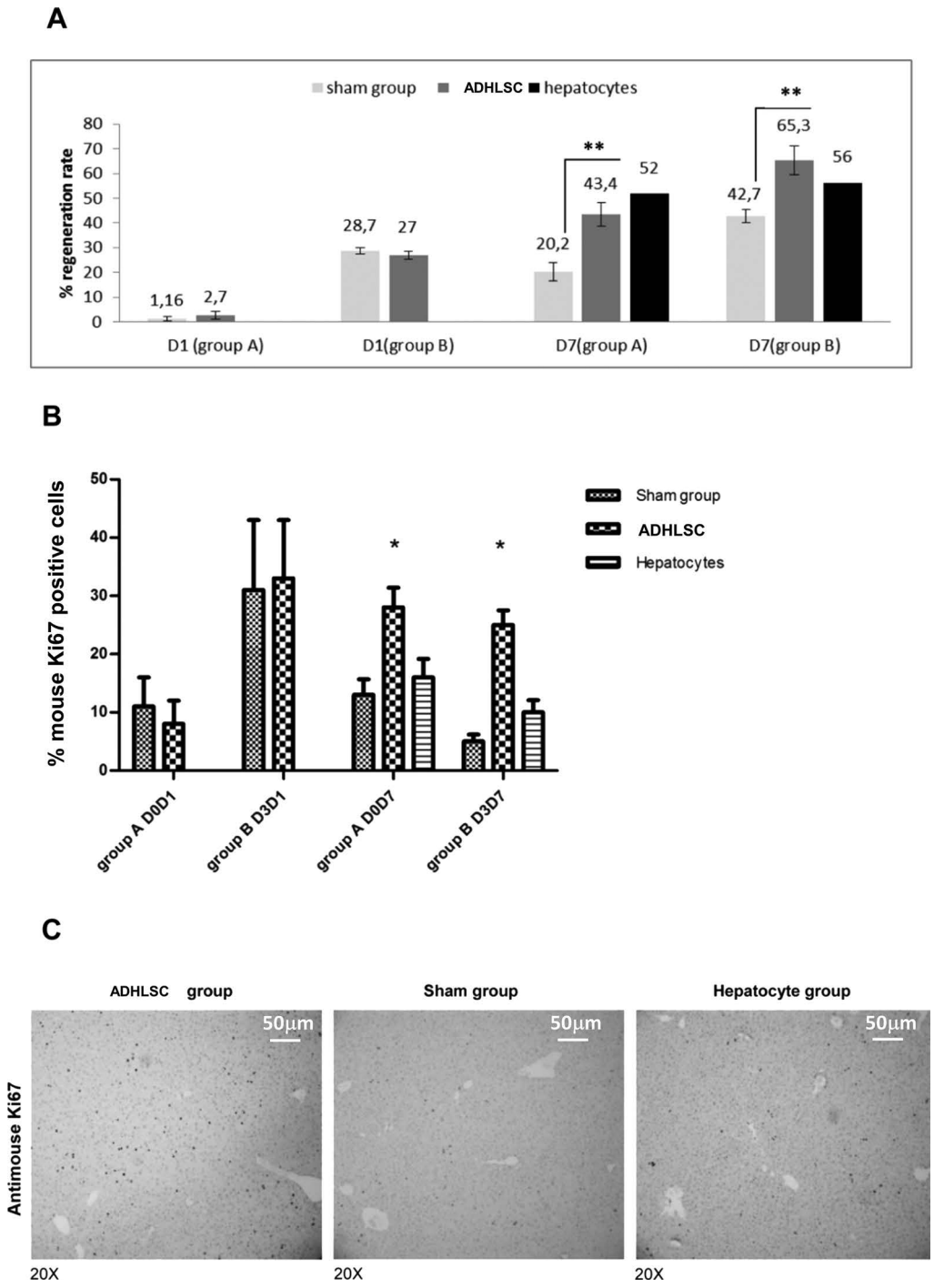

Figure 6. Hepatic regeneration evaluated through the measurement of weight and cell proliferation in mouse liver tissue. (A) Hepatic liver regeneration was evaluated using the weight of the remnant liver based on the formula described in Materials and Methods. The mouse liver regeneration observed 1 week after transplantation was more rapid and extensive in those transplanted with ADHLSCs than in those transplanted with hepatocytes or mice in the sham group. (B) Quantification of murine Ki-67$^+$ cells with ImageJ software in mice transplanted with hepatocytes and ADHLSCs compared to the sham group. Liver sections from mice transplanted with ADHLSCs and the sham group were analyzed on days 1 and 7 following transplantation (only on day 7 for hepatocytes). One day after transplantation, there was no difference between the groups. Seven days after transplantation, the percentage of mouse cells positively stained for Ki-67 was significantly higher in the ADHLSC-transplanted mice than in the sham group or the hepatocyte-transplanted mice, in both groups A and B. Results from the immunostainings in group B are displayed in (C). (C) Representative result of the anti-mouse Ki-67 immunostaining obtained on day 7 in group B, the sham group and the hepatocyte-injected group. ADHLSCs adult-derived human liver stem/progenitor cells.

the antiapoptotic, immunomodulating, and regenerative effects observed with cell therapy could result from trophic molecules secreted by mesenchymal stem cells (9,27,36,38). In this setting, we found that undifferentiated ADHLSCs had not yet fully differentiated into hepatocytes at day 7 posttransplantation and had likely not yet proliferated due to the short time period from engraftment to sacrifice. Indeed, despite albumin expression, ADHLSCs were still negative for mature hepatocyte markers such as OTC. In our previous study using a 20% hepatectomy model (16), proliferating human cells were, in fact, evidenced at later time points (1–2 months posttransplantation). Despite the fact that the transplanted human cells were not yet proliferating at the early time point in our present investigation, ADHLSCs were nonetheless able to improve mouse hepatocyte proliferation and liver regeneration very early after infusion. Taken together, these results suggest that ADHLSCs could stimulate liver regeneration to a higher extent via a paracrine effect than through their own participation in mouse liver regeneration.

One could argue that ADHLSCs are a mixed population and therefore different cell types could be playing a role in tissue regeneration. Although it is true that the cell population is heterogeneous, it has to be noted that the cells used in the experiment are not the liver cell suspension obtained directly after collagenase digestion but cells that have been expanded in vitro for four to six passages. Expansion of the parenchymal fraction in vitro and passaging of the cells allow for the enrichment of the progenitor cell population. Hepatocytes quickly dedifferentiate and die following culture in a medium other than a "long-term" medium designed to support their survival (25). Quality control testing performed on ADHLSCs have shown that they no longer express mature hepatocyte markers such as OTC or CK18, nor do they express the biliary marker CK19, or hematopoietic markers such as CD117 or CD133 (21). Further, our attempts to cultivate duct cells and sinusoidal endothelial cells suggest that they would not thrive under progenitor cell culture conditions. Even if stellate cells are found mainly in the nonparenchymal fraction, a contamination of the parenchymal fraction by these cells cannot be ruled out. However, we have demonstrated that ADHLSCs at the passage studied differ from hepatic stellate cells (2,29). Oval cells, bipotential cells that express CK19 and are capable of differentiating toward both biliary and hepatocytic lineages, could also potentially be present in the cell culture. However, our research has shown that ADHLSCs are negative for CK19. It is nonetheless true that ADHLSCs, like other MSCs, present some degree of heterogeneity, probably due in part to the fact that they arise from a plate and wait method rather than a clonal expansion. However, studies have shown that even clonal populations derived from one single cell show morphological and functional heterogeneity (31). The causes for this heterogeneity are not yet fully understood. Further research will be needed to unravel the precise mechanisms involved and modify the culture process so as to increase the homogeneity of the population. For example, Huch et al. have described a 3D organoid system allowing the clonal expansion of genome-stable bipotent stem cells from adult human liver. This system could be applied to other stem cell types (13).

In conclusion, this study demonstrates that engrafting human cells in a 70% hepatectomy murine model is more effective when the cells are infused via the intrasplenic route 3 days posthepatectomy. Moreover, engrafted undifferentiated ADHLSCs were found to stimulate mouse liver regeneration in this model, most likely through a paracrine effect. Considering the significant self-renewal potential of ADHLSCs, which still remains intact after cryopreservation, along with their capacity to engraft and differentiate in liver tissues (16), these cells likely constitute a promising therapeutic tool for liver cell therapy and repair, particularly in the context of extensive hepatectomies conducted in liver cancer patients.

ACKNOWLEDGMENTS: This study was supported by both the Région Wallonne, as part of the Regenestem project (Convention No. 1017264), and the Université Catholique de Louvain. The authors would like to thank Jonathan Evraerts and Charles de Pierpont for their technical help, and Dr. Julie Sainz for reviewing the manuscript. The authors declare no conflicts of interest.

REFERENCES

1. Azuma, H.; Paulk, N.; Ranade, A.; Dorrell, C.; Al-Dhalimy, M.; Ellis, E.; Strom, S.; Kay, M. A.; Finegold, M.; Grompe, M. Robust expansion of human hepatocytes in Fah-/-/Rag2-/-/Il2rg-/- mice. Nat. Biotechnol. 25(8):903–910; 2007.
2. Berardis, S.; Lombard, C.; Evraerts, J.; El Taghdouini, A.; Rosseels, V.; Sancho-Bru, P.; Lozano, J. J.; van Grunsven, L.; Sokal, E.; Najimi, M. Gene expression profiling and secretome analysis differentiate adult-derived human liver stem/progenitor cells and human hepatic stellate cells. PLoS One 9(1):e86137; 2014.
3. Bustin, S. A.; Benes, V.; Garson, J. A.; Hellemans, J.; Huggett, J.; Kubista, M.; Mueller, R.; Nolan, T.; Pfaffl, M. W.; Shipley, G. L.; Vandesompele, J.; Wittwer, C. T. The MIQE guidelines: Minimum information for publication of quantitative real-time PCR experiments. Clin. Chem. 55(4):611–622; 2009.
4. Cheng, K.; Benten, D.; Bhargava, K.; Inada, M.; Joseph, B.; Palestro, C.; Gupta, S. Hepatic targeting and biodistribution of human fetal liver stem/progenitor cells and adult hepatocytes in mice. Hepatology 50(4):1194–1203; 2009.
5. Chicha, L.; Tussiwand, R.; Traggiai, E.; Mazzucchelli, L.; Bronz, L.; Piffaretti, J. C.; Lanzavecchia, A.; Manz, M. G. Human adaptive immune system Rag2-/-gamma(c)-/- mice. Ann. NY Acad. Sci. 1044:236–243; 2005.
6. Ding, B. S.; Nolan, D. J.; Butler, J. M.; James, D.; Babazadeh, A. O.; Rosenwaks, Z.; Mittal, V.; Kobayashi, H.; Shido, K.; Lyden, D.; Sato, T. N.; Rabbany, S. Y.; Rafii, S. Inductive angiocrine signals from sinusoidal

endothelium are required for liver regeneration. Nature 468(7321):310–315; 2010.
7. Dokmak, S.; Fteriche, F. S.; Borscheid, R.; Cauchy, F.; Farges, O.; Belghiti, J. 2012 Liver resections in the 21st century: We are far from zero mortality. HPB 15(11): 908–915; 2013.
8. Fisher, R. A.; Strom, S. C. Human hepatocyte transplantation: Worldwide results. Transplantation 82(4):441–449; 2006.
9. Fouraschen, S. M.; Pan, Q.; de Ruiter, P. E.; Farid, W. R.; Kazemier, G.; Kwekkeboom, J.; Ijzermans, J. N.; Metselaar, H. J.; Tilanus, H. W.; de Jonge, J.; van der Laan, L. J. Secreted factors of human liver-derived mesenchymal stem cells promote liver regeneration early after partial hepatectomy. Stem Cells Dev. 21(13):2410–2419; 2012.
10. Germani, G.; Theocharidou, E.; Adam, R.; Karam, V.; Wendon, J.; O'Grady, J.; Burra, P.; Senzolo, M.; Mirza, D.; Castaing, D.; Klempnauer, J.; Pollard, S.; Paul, A.; Belghiti, J.; Tsochatzis, E.; Burroughs, A. K. Liver transplantation for acute liver failure in Europe: Outcomes over 20 years from the ELTR database. J. Hepatol. 57(2):288–296; 2012.
11. Guha, C.; Parashar, B.; Deb, N. J.; Garg, M.; Gorla, G. R.; Singh, A.; Roy-Chowdhury, N.; Vikram, B.; Roy-Chowdhury, J. Normal hepatocytes correct serum bilirubin after repopulation of Gunn rat liver subjected to irradiation/partial resection. Hepatology 36(2):354–362; 2002.
12. Hammond, J. S.; Gilbert, T. W.; Howard, D.; Zaitoun, A.; Michalopoulos, G.; Shakesheff, K. M.; Beckingham, I. J.; Badylak, S. F. Scaffolds containing growth factors and extracellular matrix induce hepatocyte proliferation and cell migration in normal and regenerating rat liver. J. Hepatol. 54(2):279–287; 2011.
13. Huch, M.; Gehart, H.; van Boxtel, R.; Hamer, K.; Blokzijl, F.; Verstegen, M. M.; Ellis, E.; van Wenum, M.; Fuchs, S. A.; de Ligt, J.; van de Wetering, M.; Sasaki, N.; Boers, S. J.; Kemperman, H.; de Jonge, J.; Izermans, J. N.; Nieuwenhuis, E. E.; Hoekstra, R.; Strom, S.; Vries, R. R.; van der Laan, L. J.; Cuppen, E.; Clevers, H. Long-term culture of genome-stable bipotent stem cells from adult human liver. Cell 160(1–2):299–312; 2015.
14. Jarnagin, W. R.; Gonen, M.; Fong, Y.; DeMatteo, R. P.; Ben-Porat, L.; Little, S.; Corvera, C.; Weber, S.; Blumgart, L. H. Improvement in perioperative outcome after hepatic resection: Analysis of 1,803 consecutive cases over the past decade. Ann. Surg. 236(4):397–406; discussion 406–397; 2002.
15. Kamiyama, T.; Nakanishi, K.; Yokoo, H.; Kamachi, H.; Tahara, M.; Yamashita, K.; Taniguchi, M.; Shimamura, T.; Matsushita, M.; Todo, S. Perioperative management of hepatic resection toward zero mortality and morbidity: Analysis of 793 consecutive cases in a single institution. J. Am. Coll. Surg. 211(4):443–449; 2010.
16. Khuu, D. N.; Nyabi, O.; Maerckx, C.; Sokal, E.; Najimi, M. Adult human liver mesenchymal stem/progenitor cells participate to mouse liver regeneration after hepatectomy. Cell Transplant. 22(8):1369–1380; 2013.
17. Lautt, W. W. Mechanism and role of intrinsic regulation of hepatic arterial blood flow: Hepatic arterial buffer response. Am. J. Physiol. 249(5 Pt 1):G549–G556; 1985.
18. Li, J.; Liang, L.; Ma, T.; Yu, X.; Chen, W.; Xu, G.; Liang, T. Sinusoidal microcirculatory changes after small-for-size liver transplantation in rats. Transpl. Int. 23(9):924–933; 2010.
19. Makino, H.; Togo, S.; Kubota, T.; Morioka, D.; Morita, T.; Kobayashi, T.; Tanaka, K.; Shimizu, T.; Matsuo, K.; Nagashima, Y.; Shimada, H. A good model of hepatic failure after excessive hepatectomy in mice. J. Surg. Res. 127(2):171–176; 2005.
20. Michalopoulos, G. K. Liver regeneration after partial hepatectomy: Critical analysis of mechanistic dilemmas. Am. J. Pathol. 176(1):2–13; 2010.
21. Najimi, M.; Khuu, D. N.; Lysy, P. A.; Jazouli, N.; Abarca, J.; Sempoux, C.; Sokal, E. M. Adult-derived human liver mesenchymal-like cells as a potential progenitor reservoir of hepatocytes? Cell Transplant. 16(7):717–728; 2007.
22. Newberry, E. P.; Kennedy, S. M.; Xie, Y.; Luo, J.; Stanley, S. E.; Semenkovich, C. F.; Crooke, R. M.; Graham, M. J.; Davidson, N. O. Altered hepatic triglyceride content after partial hepatectomy without impaired liver regeneration in multiple murine genetic models. Hepatology 48(4):1097–1105; 2008.
23. Ninomiya, M.; Shirabe, K.; Terashi, T.; Ijichi, H.; Yonemura, Y.; Harada, N.; Soejima, Y.; Taketomi, A.; Shimada, M.; Maehara, Y. Deceleration of regenerative response improves the outcome of rat with massive hepatectomy. Am. J. Transplant. 10(7):1580–1587; 2010.
24. Otsuka, Y.; Duffy, J. P.; Saab, S.; Farmer, D. G.; Ghobrial, R. M.; Hiatt, J. R.; Busuttil, R. W. Postresection hepatic failure: Successful treatment with liver transplantation. Liver Transpl. 13(5):672–679; 2007.
25. Pichard, L.; Raulet, E.; Fabre, G.; Ferrini, J. B.; Ourlin, J. C.; Maurel, P. Human hepatocyte culture. Methods Mol. Biol. 320:283–293; 2006.
26. Prigent, J.; Herrero, A.; Ambroise, J.; Smets, F.; Deblandre, G. A.; Sokal, E. M. Human progenitor cell quantification after xenotransplantation in rat and mouse models by a sensitive qPCR assay. Cell Transplant. 24(8):1639–1652; 2015.
27. Puglisi, M. A.; Tesori, V.; Lattanzi, W.; Piscaglia, A. C.; Gasbarrini, G. B.; D'Ugo, D. M.; Gasbarrini, A. Therapeutic implications of mesenchymal stem cells in liver injury. J. Biomed. Biotechnol. 2011:860578; 2011.
28. Rahbari, N. N.; Garden, O. J.; Padbury, R.; Brooke-Smith, M.; Crawford, M.; Adam, R.; Koch, M.; Makuuchi, M.; Dematteo, R. P.; Christophi, C.; Banting, S.; Ustatoff, V.; Nagino, M.; Maddern, G.; Hugh, T. J.; Vauthey, J. N.; Greig, P.; Rees, M.; Yokoyama, Y.; Fan, S. T.; Nimura, Y.; Figueras, J.; Capussotti, L.; Buchler, M. W.; Weitz, J. Posthepatectomy liver failure: A definition and grading by the International Study Group of Liver Surgery (ISGLS). Surgery 149(5):713–724; 2011.
29. Raicevic, G.; Najar, M.; Najimi, M.; El Taghdouini, A.; van Grunsven, L. A.; Sokal, E.; Toungouz, M. Influence of inflammation on the immunological profile of adult-derived human liver mesenchymal stromal cells and stellate cells. Cytotherapy 17(2):174–185; 2015.
30. Rajvanshi, P.; Kerr, A.; Bhargava, K. K.; Burk, R. D.; Gupta, S. Studies of liver repopulation using the dipeptidyl peptidase IV-deficient rat and other rodent recipients: Cell size and structure relationships regulate capacity for increased transplanted hepatocyte mass in the liver lobule. Hepatology 23(3):482–496; 1996.
31. Rennerfeldt, D. A.; Van Vliet, K. J. Concise review: When colonies are not clones: Evidence and implications of intra-colony heterogeneity in mesenchymal stem cells. Stem Cells 34(5):1135–1141; 2016.

32. Sakamoto, T.; Liu, Z.; Murase, N.; Ezure, T.; Yokomuro, S.; Poli, V.; Demetris, A. J. Mitosis and apoptosis in the liver of interleukin-6-deficient mice after partial hepatectomy. Hepatology 29(2):403–411; 1999.
33. Stange, J.; Ramlow, W.; Mitzner, S.; Schmidt, R.; Klinkmann, H. Dialysis against a recycled albumin solution enables the removal of albumin-bound toxins. Artif. Organs 17(9):809–813; 1993.
34. Stephenne, X.; Nicastro, E.; Eeckhoudt, S.; Hermans, C.; Nyabi, O.; Lombard, C.; Najimi, M.; Sokal, E. Bivalirudin in combination with heparin to control mesenchymal cell procoagulant activity. PLoS One 7(8):e42819; 2012.
35. Stephenne, X.; Vosters, O.; Najimi, M.; Beuneu, C.; Dung, K. N.; Wijns, W.; Goldman, M.; Sokal, E. M. Tissue factor-dependent procoagulant activity of isolated human hepatocytes: Relevance to liver cell transplantation. Liver Transpl. 13(4):599–606; 2007.
36. Stock, P.; Bruckner, S.; Ebensing, S.; Hempel, M.; Dollinger, M. M.; Christ, B. The generation of hepatocytes from mesenchymal stem cells and engraftment into murine liver. Nature Protoc. 5(4):617–627; 2010.
37. Turner, R. A.; Wauthier, E.; Lozoya, O.; McClelland, R.; Bowsher, J. E.; Barbier, C.; Prestwich, G.; Hsu, E.; Gerber, D. A.; Reid, L. M. Successful transplantation of human hepatic stem cells with restricted localization to liver using hyaluronan grafts. Hepatology 57(2):775–784; 2013.
38. van Poll, D.; Parekkadan, B.; Cho, C. H.; Berthiaume, F.; Nahmias, Y.; Tilles, A. W.; Yarmush, M. L. Mesenchymal stem cell-derived molecules directly modulate hepatocellular death and regeneration in vitro and in vivo. Hepatology 47(5):1634–1643; 2008.
39. Weber, A.; Groyer-Picard, M. T.; Franco, D.; Dagher, I. Hepatocyte transplantation in animal models. Liver Transpl. 15(1):7–14; 2009.
40. Yokoyama, Y.; Nimura, Y.; Nagino, M.; Bland, K. I.; Chaudry, I. H. Role of thromboxane in producing hepatic injury during hepatic stress. Arch. Surg. 140(8):801–807; 2005.